*American Mineralogist, Volume 78, pages 1192–1196, 1993*

# Crystal structure and compressibility of 3:2 mullite

**Davor Balzar,* Hassel Ledbetter**

Materials Science and Engineering Laboratory, National Institute of Standards and Technology, Boulder, Colorado 80303, U.S.A.

## Abstract

The crystal structure of 3:2 mullite ($3Al_2O_3 \cdot 2SiO_2$) has been refined by Rietveld refinement of X-ray powder diffraction data. The average structure is described successfully by previously published models for 2:1 mullite. Bond lengths of tetrahedral cations are slightly shorter, because of the smaller ionic radii of $Si^{4+}$ relative to $Al^{3+}$. Using ultrasonic methods, we determined the bulk modulus (reciprocal compressibility). The result, 174 GPa, is slightly lower than that of a prediction based on a rigid-ion ionic crystal model: 190 GPa.

## Introduction

Molar volume $V$ and compressibility represent two of the basic cohesive properties of a solid, binding energy being the third. Many physical properties depend on volume; for example, the bulk modulus $B$ varies as $V^{-\frac{1}{3}}$(Gilman, 1969). From the elastic constants and volume, we can calculate one of the most basic properties of a solid: the Debye characteristic temperature (Blackman, 1955).

As summarized by Skoog and Moore (1988), the elastic properties of mullite remain poorly characterized. They give a bulk modulus of 91 GPa, astonishingly low when compared with values for $\alpha$ alumina, 252 GPa (Tefft, 1966), and fused silica, 37 GPa (Bogardus, 1965). A rule-of-mixture approximation gives 166 GPa. For stishovite, the stiffest polymorph of silica, both measurement and theory (first principle, ab initio, quantum mechanical) give a bulk modulus of about 300 GPa (Keskar et al., 1991).

The crystal structure of mullite was studied thoroughly by Sadanaga et al. (1962), Burnham (1963, 1964), Ďurovič (1969), Angel and Prewitt (1986), and Angel et al. (1991). Mullite is intermediate in composition between alumina ($Al_2O_3$) and sillimanite ($Al_2SiO_5$). It is usually represented by the formula $Al_2Al_{2+2x}Si_{2-2x}O_{10-x}$, where $x$ denotes the fraction of vacancies per unit cell. Ordering of O vacancies, and possibly of the tetrahedral cation sites, causes an incommensurate modulation of structure that varies with composition (Cameron, 1977a). Nevertheless, the average structure can be described satisfactorily in space group *Pbam* with $Z = 1$. Although the previous crystal structure studies were done on the alumina-rich compounds with $x \approx 0.40$ (2:1 mullite), structural parameters should change smoothly toward both silica-rich and alumina-rich compositions. Ďurovič and Fejdi (1976), for instance, found that $1.54Al_2O_3 \cdot GeO_2$ is isostructural with silica mullite.

Here we report the crystal structure and compressibility (reciprocal bulk modulus) of 3:2 mullite: $3Al_2O_3 \cdot 2SiO_2$. We augment the compressibility measurement with a rigid-ion ionic crystal model calculation. Input to this calculation includes ionic positions and charges.

## Experiments and calculations

### X-ray diffraction

We used a bulk specimen of hot-pressed submicrometer mullite powder synthesized by Mizuno and Saito (1989). The specimen surface was mechanically polished and finished with 1-$\mu$m diamond grinding.

Cu$K\alpha$ X-ray diffraction data were acquired in the range 20–160° ($2\theta$) counting 10 s every 0.02° ($2\theta$). A standard $\theta$-$2\theta$ powder diffractometer with incident-beam and diffracted-beam Soller slits and a Ge solid state detector were used. With 2-mm incident slits, the beam was entirely contained in the specimen surface at the lowest angles of interest.

Because preliminary X-ray diffraction scans of the specimen showed relatively limited preferred orientation, we refined the X-ray diffraction pattern with the Rietveld program GSAS (Larson and Von Dreele, 1988). The starting model followed single-crystal results of Angel and Prewitt (1986). Six parameters of the cosine Fourier series background were refined. Pseudo-Voigt peak shapes (Thompson et al., 1987) were assumed with anisotropic peak broadening (Greaves, 1985). The March-Dollase preferred-orientation correction (Dollase, 1986) along [001] was used.

### Compressibility

We used a pulse echo superposition method described by Ledbetter et al. (1980). We used 9-MHz $x$-cut and $ac$-cut quartz transducers bonded with phenyl salicylate. Ultrasonic waves were reflected from flat and parallel surfaces of a polycrystalline specimen hot-pressed into the shape of rectangular parallelepiped measuring 8 × 18 × 30 mm. Sound velocities were determined by the rela-

* On leave from the Physics Department, Faculty of Metallurgy, University of Zagreb, 44000 Sisak, Croatia.

0003–004X/93/1112–1192$02.00

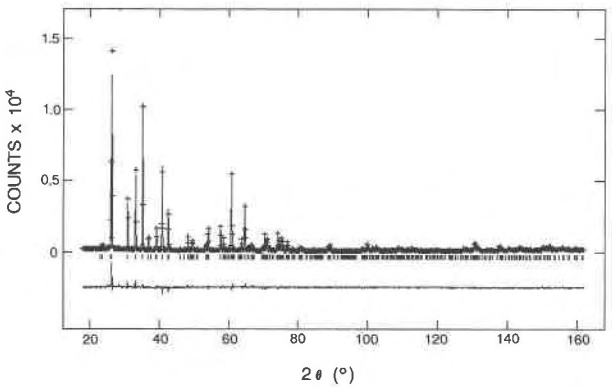


Fig. 1. Rietveld pattern refinement of 3:2 mullite. Observed points are presented with crosses, and the calculated pattern is shown with a full line. The difference pattern is shown at the bottom. Short vertical markers represent allowed reflections.

tionship

$$v = 2l/t. \tag{1}$$

Here $l$ denotes specimen thickness and $t$ round-trip transit time for an ultrasonic wave. These velocities convert to elastic stiffnesses $C$ by the usual formula.

$$C = \rho v^2. \tag{2}$$

Here $\rho$ denotes mass density, 3.156 g/cm$^3$, determined by Archimedes' method, using distilled $H_2O$ as a standard. To calculate the void volume fraction $f_V$, we used the relationship

$$f_V = 1 - \rho/\rho_{\text{X-ray}}. \tag{3}$$

The bulk modulus depends on two sound velocities, longitudinal and transverse:

$$B = \rho(v_l^2 - 4v_t^2/3). \tag{4}$$

From our experience in measuring elastic properties of standard materials, we estimate the error in $B$ as less than 5:1000.

### Ionic-model calculation

In a Born model, the total Madelung (electrostatic, ionic) energy $E_i$ relates simply to the total cohesive energy $E_c$ (Brown, 1967):

$$E_c = -E_i(1 - 1/n). \tag{5}$$

Here, $n$ denotes the Born repulsive exponent. In the same model, we can calculate the bulk modulus (reciprocal compressibility):

$$B = -\frac{E_i}{9V_0}(n - 1). \tag{6}$$

Here, $V_0$ denotes the average atomic volume, determined by dividing the unit-cell volume by the number of atoms in the cell. The electrostatic energy is given by

**Table 1.** Crystallographic data and refinement-reliability factors for 3:2 mullite

| | |
|---|---|
| Space group: *Pbam*, $Z = 1$ | $R_{wp}$* = 0.103 |
| $a$ = 7.54336(6) Å | $R_p$** = 0.079 |
| $b$ = 7.69176(6) Å | $R_B$† = 0.077 |
| $c$ = 2.88402(2) Å | $\chi^2$ = 2.74 |
| $V$ = 167.335(2) Å$^3$ | Preferred-orientation coeff. $M$ (001) = 0.900(2) (Without texture, $M$ = 1.0) |

*Note:* estimated standard deviations are given in parentheses.
* $R_{wp} = [\Sigma w(I_o - I_c)^2/\Sigma wI_o^2]^{1/2}$.
** $R_p = \Sigma|I_o - I_c|/\Sigma I_o$ (whole pattern).
† $R_B = \Sigma|I_o - I_c|/\Sigma I_o$ (Bragg intensities only).

$$E_i = -(Ze)^2\frac{M_a}{a}. \tag{7}$$

Here $e$ denotes electron charge, $Z$ the largest common factor of various pointlike ionic charges $Ze$, and $a$ the characteristic unit-cell length. (The choice of $a$ is arbitrary. Comparing Eqs. 6–8 shows that $a$ disappears from the energy and bulk-modulus expressions.) We can obtain the nondimensional Madelung constant $M$ by summing over all sites in the unit cell:

$$M_a = -\frac{a}{2n}\sum_j q_j p_j \Phi_j. \tag{8}$$

Here, $N$ denotes the number of molecules per unit cell, $q_j$ the charge on ion $j$, $p_j$ the number of $j$-ion sites in the unit cell, and $\Phi_j$ the site self potential. To calculate the lattice self potentials, we used Ewald's method, as formulated by Tosi (1954) and described by van Gool and Piken (1969). To verify our computer program, which resembles closely the program by van Gool and Piken, we calculated Madelung constants for all the crystal structures listed by Tosi; for all cases, we reproduced his results.

For most oxides, $n$ varies between 4 and 5 (Anderson and Anderson, 1970). For mullite, we took $n = 3.14$, the 3:2 weighted average of $n = 4.17$ ($\alpha$ alumina) and 1.59 (fused silica). We determined these $n$ values from Equation 6 and the elastic constants measured by Bogardus (1965) and Tefft (1966). Following Equation 5, $E_i$ accounts for approximately 70% of the cohesion.

## Results and discussion

The X-ray powder diffraction pattern is shown in Figure 1, and results of the refinement in Tables 1 and 2. The diffraction pattern showed only one very weak impurity line at 28.47° and no superlattice reflections, which are very diffuse for siliceous mullite (Cameron, 1977b). Mizuno and Saito (1989) reported the weight ratio of $Al_2O_3$ to $SiO_2$ as 2.56, which is almost equal to the expected value of 2.55 for 3:2 mullite. Moreover, their chemical analysis showed the total amount of impurities to be <0.1 wt%. In particular, the $Fe_2O_3$ content was 0.03 wt%, and no $TiO_2$ was detected. Both oxides usually occur with mullite, which absorbs Fe and Ti in its structure (Cameron, 1977b). According to Cameron, the $a$ lattice

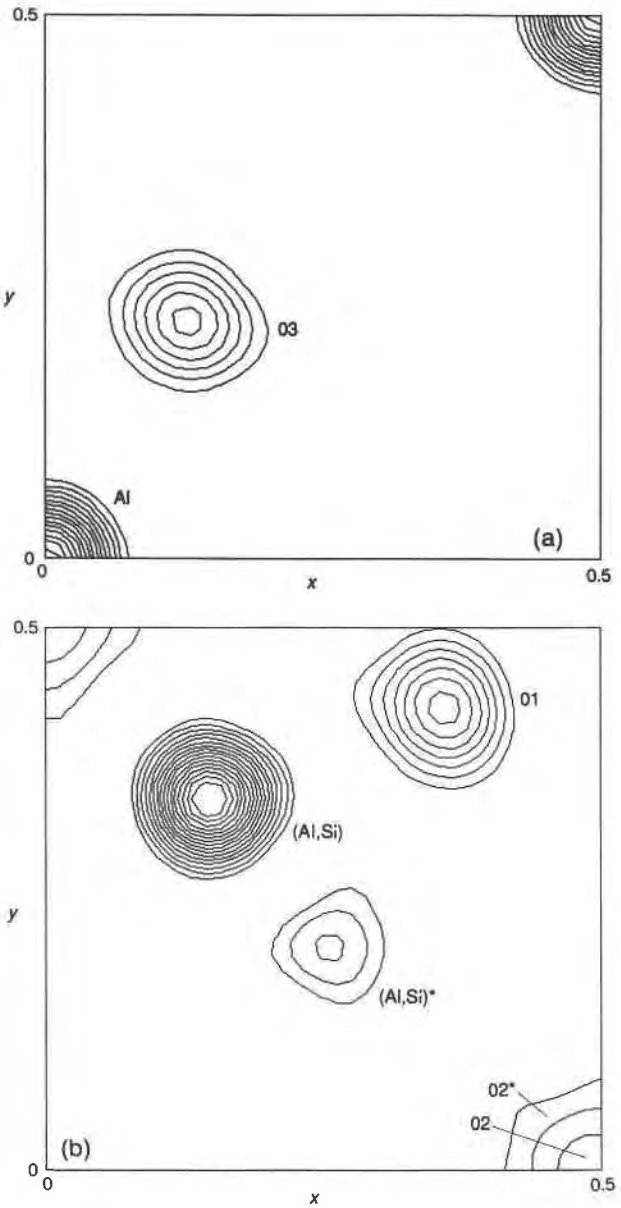


Fig. 2. Final calculated Fourier maps parallel to (001): (**a**) $z = 0$. Contours are drawn at 3–45 e/Å$^3$, every 3 e/Å$^3$; (**b**) $z = ½$. Contours are drawn at 2.5–40 e/Å$^3$, every 2.5 e/Å$^3$.

parameter can be correlated with the chemical composition of mullite. From our Table 1 and Figure 3 of Cameron, the ratio 3:2 follows for our specimen. Furthermore, by correlating the $a$ cell parameter with the cell volume, from Figure 2 of Cameron, we estimate the Fe and Ti content of our specimen as $<1$ wt%. Attempts to refine the occupancy factors of Fe and Ti on Al octahedral sites failed, confirming further that the possible substitution of Al by Fe and Ti is negligible.

During the refinement, occupancies of the partially occupied cation sites were fixed at values corresponding to the assumed 3:2 mullite composition ($x = 0.25$) with the (Al,Si)* site occupied only by Si. Because of similar scattering factors of Al and Si, strong correlation of their parameters did not allow for the simultaneous refinement of their occupancy factors. We first constrained the (Al,Si) site to $1 - x/2 = 0.875$ occupancy, and refined relative amounts of Al and Si. In the last step, both Al and Si were allowed to interchange between $^{[4]}$(Al,Si) and $^{[4]}$(Al,Si)* sites. This caused a temperature factor to be negative and slight overpopulation of the (Al,Si)* site. However, in view of the similar scattering power of Al and Si atoms, low occupancy of the particular site, and powder diffraction experiment, reported standard deviations of occupancies from Table 2 seem to be underestimated. Even the single-crystal study of germanium mullite (Ďurovič and Fejdi, 1976) give ambiguous relative occupancies of the (Al,Si)* site. Total O occupancy converged without constraints to a value of 9.742(13), very close to the expected value of 9.75 for 3:2 mullite. However, similar to results for the (Al,Si)* site, for the O2* site we find an unreliable temperature factor and too many O atoms, compared with the O2 site; theoretically, the occupancy ratio O2/O2* should be $(1 - 3x/2)/(x/2)$.

Figure 2 shows final calculated Fourier maps parallel to (001) at $z = 0$ and $z = ½$. The electron densities of the O1 and O3 sites are elongated along the direction connecting two tetrahedral sites (Burnham, 1964; Angel and Prewitt, 1986) because the O atoms have slightly different positions when coordinating (Al,Si) or (Al,Si)* sites.

Table 3 gives bond lengths and angles for 3:2 mullite. There is no significant difference in bond lengths from the results of Ďurovič (1969) for 1.83:1 mullite, but tetrahedral bond lengths are shorter compared with the values published by Burnham (1963, 1964) and Angel and

**Table 2.** Refined structure parameters for 3:2 mullite

| Atom | Site | $x$ | $y$ | $z$ | $B_{iso}$ (Å$^2$) | Occupancy |
|---|---|---|---|---|---|---|
| Al | 2a | 0 | 0 | 0 | 0.23(3) | 1 |
| (Al,Si) | 4h | 0.1485(1) | 0.3407(1) | ½ | 0.24(2) | 0.525(2),0.342(2) |
| (Al,Si)* | 4h | 0.2610(7) | 0.2073(7) | ½ | 0.00(10) | 0.100(2),0.033(2) |
| O1 | 4h | 0.3577(2) | 0.4235(2) | ½ | 2.12(4) | 1 |
| O2 | 2d | ½ | 0 | ½ | 2.06(18) | 0.475(10) |
| O2* | 4h | 0.4635(20) | 0.0465(18) | ½ | 4.53(36) | 0.198(6) |
| O3 | 4g | 0.1265(2) | 0.2197(2) | 0 | 2.16(4) | 1 |

*Note:* estimated standard deviations are given in parentheses. Because some O is absent from the structure, some of the $^{[4]}$(Al,Si) cations are displaced to the (Al,Si)* site, and some of the O ions are displaced from the symmetry center at $x = ½$, $y = 0$, $z = ½$ to the O2* site.

**TABLE 3.** Bond lengths and angles for 3:2 mullite

| Bond lengths (Å) | | Bond angles (°) | |
|---|---|---|---|
| | | **Octahedron $AlO_6$** | |
| Al-O1 × 4 | 1.892(1) | O1-Al-O1 × 2 | 99.34(9) |
| | | O1-Al-O1 × 2 | 80.66(9) |
| | | O1-Al-O1 × 2 | 180 |
| Al-O3 × 2 | 1.941(2) | O1-Al-O3 × 4 | 89.53(6) |
| | | O1-Al-O3 × 4 | 90.47(6) |
| | | O3-Al-O3 × 1 | 180 |
| | | **Tetrahedron $(Al,Si)O_4$** | |
| (Al,Si)-O1 × 1 | 1.701(2) | O1-(Al,Si)-O2 × 1 | 110.47(8) |
| | | O1-(Al,Si)-O3 × 2 | 106.95(8) |
| (Al,Si)-O2 × 1 | 1.660(1) | O2-(Al,Si)-O3 × 2 | 109.47(7) |
| (Al,Si)-O3 × 2 | 1.724(1) | O3-(Al,Si)-O3 × 1 | 113.49(11) |
| | | **Tetrahedron $(Al,Si)^*O_4$** | |
| (Al,Si)*-O1 × 1 | 1.816(5) | O1-(Al,Si)*-O2* × 1 | 105.3(5) |
| | | O1-(Al,Si)*-O3 × 2 | 100.43(21) |
| (Al,Si)*-O2* × 1 | 1.965(15) | O2*-(Al,Si)*-O3 × 2 | 118.74(23) |
| (Al,Si)*-O3 × 2 | 1.766(3) | O3 -(Al,Si)*-O3 × 1 | 109.49(30) |

*Note:* estimated standard deviations are given in parentheses.

Prewitt (1986) for 1.92:1 mullite. This is expected because for silica-rich mullite the smaller size of $Si^{4+}$ compared with $Al^{3+}$ causes a decrease in the average bond length of tetrahedral cations. The distance (Al,Si)*-O2* seems too long, however. Probably the O2* positional parameters are less accurate because of the strong correlation between O structural parameters and the low occupancy of the particular O site.

The compressibility, or bulk modulus, is now considered. Our measured value, $B$ = 174 GPa, differs from those of previous reports (Skoog and Moore, 1988) but seems reasonable. Above, the rule-of-mixture approximation was mentioned: 166 GPa. We can make a more realistic approximation by using Anderson's (1969) suggestion that for complex oxides the squared bulk-modulus velocities $v_b$ add linearly:

$$v_b^2 = \sum_i f(i) v_b^2(i). \quad (9)$$

Here, $i$ denotes the component and $f_i$ the molecular fraction. Thus, $f_{Al_2O_3} = 0.6$, $f_{SiO_2} = 0.4$, $v_{b,\,Al_2O_3} = 0.795$ cm/$\mu$s. Because silica shows so many polymorphic forms, the value of $v_{b,\,SiO_2}$ is uncertain. For fused-silica, $v_{b,\,SiO_2} = 0.384$ cm/$\mu$s (Bogardus, 1965). For stishovite, $v_{b,\,SiO_2} = 0.836$ cm/$\mu$s (Keskar et al., 1991). Using the relation $B = \rho v_b^2$, the lower value gives $B$ = 126 GPa, the higher 208 GPa. This result suggests strongly that the Si-O bond strength in mullite is much closer to that in stishovite than that in $\alpha$ quartz, even though the Si-O coordination remains approximately tetrahedral.

Further support for a greater bulk modulus comes from the ionic crystal model calculation described above. The result, $B$ = 190 GPa, is about 10% higher than observation, approximately the uncertainty of the calculation, especially for a nonsimple crystal structure. In this case, nonsimple means shared Al-Si cation sites and incommensurate structural modulation. The latter would cause a decrease in the elastic stiffness. Thus, the intrinsic elastic modulus may be closer to 190 than to 174 GPa. We did a similar calculation for sillimanite, $Al_2O_3 \cdot SiO_2$, where the crystal structure is less ambiguous. Using the published atomic positions (Winter and Ghose, 1979) we found $B_{sillimanite}$ = 139 GPa, this lower value reflecting a higher fraction of the softer $SiO_2$. A naive linear rule-of-mixture estimate using $B_{fused\ silica}$ gives $B_{sillimanite}$ = 145 GPa. Apparently, $B_{sillimanite}$ remains nonmeasured. Such a measurement would help enormously in understanding Si-O bonds in sillimanite.

## CONCLUSIONS

We report refinement of the average crystal structure of 3:2 mullite by using Rietveld powder methods. Results agree with the previously published single-crystal studies of 2:1 mullite. Because of strong correlation between the occupancies of two tetrahedral cation sites, it is difficult to conclude how many Si atoms reside statistically on the additional (Al,Si)* site. As expected, tetrahedral bond lengths are slightly shorter than for 2:1 mullite, because of the difference in ionic sizes of $Si^{4+}$ and $Al^{3+}$.

Using refined atomic positions, we calculated the bulk modulus using a rigid-ion ionic crystal model. The result, $B$ = 190 GPa, is somewhat higher than the ultrasonically measured value of 174 GPa. Moreover, a simple rule-of-mixture approximation gives 166 GPa. Hence, we conclude that the reported bulk modulus of 91 GPa (Skoog and Moore, 1988) is too low.

## ACKNOWLEDGMENTS

W. Kriven, University of Illinois (Urbana), provided the mullite specimen. S. Kim, NIST (Boulder), helped with measurements and calculations.

## REFERENCES CITED

Anderson, D. (1969) Bulk modulus–density systematics. Journal of Geophysical Research, 74, 3857–3864.

Anderson, D., and Anderson, O. (1970) The bulk-modulus-volume relationship for oxides. Journal of Geophysical Research, 75, 3494–3500.

Angel, R.J., and Prewitt, C.T. (1986) Crystal structure of mullite: A reexamination of the average structure. American Mineralogist, 71, 1476–1482.

Angel, R.J., McMullan, R.K., and Prewitt, C.T. (1991) Substructure and superstructure of mullite by neutron diffraction. American Mineralogist, 76, 332–342.

Blackman, M. (1955) The specific heat of solids. In Handbuch der Physik, vol. VII, part 1, p. 325–382. Springer-Verlag, Berlin.

Bogardus, E. (1965) Third-order elastic constants of Ge, MgO, and fused $SiO_2$. Journal of Applied Physics, 36, 2504–2513.

Brown, F. (1967) The physics of solids, 105 p. Benjamin, New York.

Burnham, C.W. (1963) The crystal structure of mullite. Carnegie Institution of Washington Year Book, 62, 158–165.

——— (1964) The crystal structure of mullite. Carnegie Institution of Washington Year Book, 63, 223–228.

Cameron, W.E. (1977a) Mullite: A substituted alumina. American Mineralogist, 62, 747–755.

——— (1977b) Composition and cell dimensions of mullite. American Ceramic Society Bulletin, 56, 1003–1011.

Dollase, W.A. (1986) Correction of intensities for preferred orientation in powder diffractometry: Application of the March model. Journal of Applied Crystallography, 19, 267–272.

Ďurovič, S. (1969) Refinement of the crystal structure of mullite. Chemicke Zvesti, 23, 113–128.

Ďurovič, S., and Fejdi, P. (1976) Synthesis and crystal structure of germanium mullite and crystallochemical parameters of D-mullites. Silikáty, 20, 97–112.

Gilman, J. (1969) Micromechanics of flow in solids, p. 29–41. McGraw-Hill, New York.

Greaves, C. (1985) Rietveld analysis of powder neutron diffraction data displaying anisotropic crystallite size broadening. Journal of Applied Crystallography, 18, 48–50.

Keskar, N.R., Troullier, N., Martins, J.L., and Chelikowsky, J.R. (1991) Structural properties of $SiO_2$ in the stishovite structure. Physical Review B, 44, 4081–4088.

Larson, A.C., and Von Dreele, R.B. (1988) GSAS: General structure analysis system. Los Alamos National Laboratory Report LAUR 86-748.

Ledbetter, H., Frederick, N., and Austin, M. (1980) Elastic-constant variability in stainless-steel 304. Journal of Applied Physics, 51, 305–309.

Mizuno, M., and Saito, H. (1989) Preparation of highly pure fine mullite powder. Journal of the American Ceramic Society, 72, 377–382.

Sadanaga, R., Tokonami, M., and Takéuchi, Y. (1962) The structure of mullite, $2Al_2O_3 \cdot SiO_2$, and relationship with the structures of sillimanite and andalusite. Acta Crystallographica, 15, 65–68.

Skoog, A., and Moore, R. (1988) Refractory of the past for the future: Mullite and its use as a bonding phase. Ceramic Bulletin, 67, 1180–1185.

Tefft, W. (1966) Elastic constants of synthetic single crystal corundum. Journal of Research of the National Bureau of Standards, 70A, 277–280.

Thompson, P., Cox, D.E., and Hastings, J.B. (1987) Rietveld refinement of Debye-Scherrer synchrotron X-ray data from $Al_2O_3$. Journal of Applied Crystallography, 20, 79–83.

Tosi, M. (1954) Cohesion of ionic solids in the Born model. Solid State Physics. 16, 1–120.

van Gool, W., and Piken, A. (1969) Lattice self potentials and Madelung constants for some compounds. Journal of Materials Science, 4, 95–104.

Winter, J.K., and Ghose, S. (1979) Thermal expansion and high-temperature crystal chemistry of the $Al_2SiO_5$ polymorphs. American Mineralogist, 64, 573–586.

Manuscript received November 2, 1992
Manuscript accepted July 17, 1993